






Detecting adverse high-order drug interactions from individual case safety reports using computational statistics on disproportionality measures

Jules Bangard ¹ Institut de Recherche Mathématique Avancée, UMR 7501 Université de Strasbourg et CNRS 7 rue René-Descartes, 67000 Strasbourg, France
Einar Holsbø  Faculty of Science and Technology, UiT-The Arctic University of Norway, PO, Box 6050 Stakkevollan, N-9037 Tromsø, Norway
Kristian Svendsen  Faculty of Health Sciences, UiT the Arctic University of Norway, Tromsø, Norway
Vittorio Perduca  CNRS, MAP5, Université Paris Cité, F-75006 Paris, France
Étienne Birmelé  Institut de Recherche Mathématique Avancée, UMR 7501 Université de Strasbourg et CNRS 7 rue René-Descartes, 67000 Strasbourg, France

Date published: 2026-01-15 Last modified: 2026-01-15

Abstract

Adverse drug interactions are a critical concern in pharmacovigilance, particularly as the controlled environment of clinical trials often lacks the scale and diversity to detect rare events or drug interactions. While spontaneous reporting systems (SRS) provide the necessary breadth for post-market surveillance, identifying these interactions within such large-scale data remains a significant computational challenge. This study introduces a computational framework for adverse drug interaction detection, leveraging disproportionality analysis on individual case safety reports. By integrating the Anatomical Therapeutic Chemical classification, the framework extends beyond drug interactions to capture hierarchical pharmacological relationships. This enables exploration of the space of drug interactions beyond pairwise interactions. To address biases inherent in existing disproportionality measures, we employ a hypergeometric risk metric, while a Markov Chain Monte Carlo algorithm provides robust empirical p-value estimation for the risk associated to cocktails. A genetic algorithm further facilitates efficient identification of high-risk drug cocktails. Validation on synthetic and FDA Adverse Event Reporting System data demonstrates the method's efficacy in detecting established drugs and drug interactions associated with myopathy-related adverse events. Implemented as an R package, this framework offers a reproducible, scalable tool for post-market drug safety surveillance.

Keywords: Disproportionality Analysis, Drug-Interactions, Genetic Algorithm, Markov Chain Monte Carlo, Pharmacovigilance, Spontaneous Reporting Systems

¹ Contents

² 1 Introduction

2

¹Corresponding author: jules.bangard@math.unistra.fr

3	2 Methods	4
4	2.1 ATC Tree and Cocktail Definition	4
5	2.2 Cocktail Risk Characterization	4
6	2.2.1 Scoring Functions in Pharmacovigilance	5
7	2.3 Distinguishing Combined Risk from True Interaction	5
8	2.4 Disproportionality Identification	6
9	2.4.1 High-risk Drug Cocktails Identification	6
10	2.4.2 Distance between drug cocktails and cocktail penalisation	7
11	2.4.3 Output clustering	8
12	2.5 Approximate P-Value Assignment for Drug Cocktails	8
13	2.6 Datasets	10
14	2.6.1 Simulated data	10
15	2.6.2 FAERS Data	10
16	3 Results	11
17	3.1 Score Comparison	11
18	3.2 Application to the Simulated Dataset	11
19	3.2.1 Estimation of Risk Distribution	11
20	3.2.2 Genetic algorithm output and clustering	14
21	3.3 Application to the FAERS Spontaneous Reporting Data	15
22	3.3.1 Estimation of Risk Distribution	15
23	3.3.2 Genetic algorithm output and clustering	15
24	4 Conclusion	17
25	Funding	19
26	5 Appendices	19
27	5.1 Appendix A : Distance Pseudo-code Algorithm	19
28	5.2 Appendix B : Calibration Under the Null	20
29	5.3 Appendix C : FAERS Clustering	20
30	5.4 Appendix D : Algorithmic Complexity	20
31	6 Code and Results	21
32	References	21
33	Session information	24

34 **1 Introduction**

35 There are inherent limitations of clinical trials (RCTs) done before a medication is authorised in
36 terms of cost, surveillance time, size and a lack of diversity of patients included (e.g. that pregnant
37 woman, children and elderly often are not included) (Sanson-Fisher et al. 2007). Another issue is
38 that RCTs are limited in their ability to detect rare adverse drug reactions (ADRs) and potential drug
39 interactions (DDIs) since they usually only include a few thousand participants at most. Moreover,
40 the use of multiple medications is often an exclusion criterion in RCTs, leaving gaps in the assessment
41 of polypharmacy risks. As a result, tested drug combinations tend to be limited to those where
42 physicians and pharmacologists have existing clinical experience or hypotheses about potential
43 interactions (Heijden et al. 2002). This means that monitoring of the safety of medications and the

44 potential for DDIs after marketing is essential. This monitoring is often referred as post-authorization
45 pharmacovigilance.

46 Elderly individuals are commonly prescribed multiple medications due to the increasing prevalence
47 of comorbidities associated with aging. One study suggested that patients aged 75 or older in Austria
48 took on average 7.5 drugs (Schuler et al. 2008). Among this demographic, 10% of hospitalizations
49 were attributed to ADRs, and 18.7% of these ADRs were caused by a combination of more than one
50 drug, a drug-drug interaction. More broadly, a meta-analysis attributed approximately 22.2% of
51 hospitalizations caused by adverse drug reactions to DDIs (Dechanont et al. 2014).

52 Disproportionality analysis (DA) encompass widely used methods in pharmacovigilance to detect
53 ADRs by assessing the frequency of adverse events (AE) associated with specific drug consumption
54 relative to what would be expected. Most established disproportionality methods like the proportional
55 reporting ratio (PRR)(Evans, Waller, and Davis 2001), reporting odds ratio (ROR)(Eugene P. van
56 Puijenbroek et al. 2002), Bayesian Confidence Propagation Neural Network (BCPNN) (Bate et al.
57 1998), and the Gamma Poisson Shrinker (GPS) (DuMouchel 1999) allow for the identification of
58 signals that warrant further investigation in the context of single drug assessment. The tree-based
59 scan statistic Heo et al. (2024) takes advantage of the tree structure of the Anatomical Therapeutic
60 Clinical (ATC) drug classification in order to allow to select a drug family rather than a single drug, a
61 family corresponding to a subtree of the ATC tree. Likelihood-ratios tests then allow to choose the
62 most relevant family.

63 In order not to overinterpret high proportions in case of rare drug cocktails, it is possible to derive
64 a score from an independence test on the contingency table counting the presence or absence of
65 the adverse event depending on the consumption of the drug cocktail. (Gosho et al. 2017) use a
66 chi-square statistic to do so, while (Ahmed et al. 2010) rather use the Fisher exact test which has the
67 advantage of being non-asymptotic.

68 Fewer DAs methods are available to use for multiple drugs consumption, such as the Ω shrinkage
69 method (Norén et al. 2008). This method allows the use of a DA measure in order to detect sets of
70 the type *Drug-Drug-Adverse Event* and stands as the standard measure when it comes to detecting
71 the interactions of two drugs. Adaptation of the PRR for a single drug has been proposed like the
72 Concomitant Signal Score (CSS) (Noguchi et al. 2020) and the PRR adaptation for DDIs (Wang et al.
73 2020).

74 Other methods than DA measures exist in order to detect DDIs. Among them, well known methods
75 encompass logistic models (Eugène P. van Puijenbroek et al. 2000; Van Puijenbroek et al. 1999)
76 and association rules methods (Noguchi et al. 2018; Ibrahim et al. 2016). One can refer to multiple
77 reviews for a more detailed overview of existing methods (Ibrahim et al. 2021; Hauben 2023).

78 Computational pharmacovigilance methods are typically applied to Spontaneous Reporting Systems
79 (SRS), which aggregate Individual Case Safety Reports (ICSRs)—real-world data submitted by health-
80 care professionals, manufacturers, and patients. Such reports contain informations about intake of
81 medications for each patients as well as their experienced AE. While SRS databases, such as the FDA
82 Adverse Event Reporting System (FAERS), provide the scale necessary to detect rare events, they
83 possess inherent limitations. These include under-reporting, where only a fraction of adverse events
84 are captured (Bate and Evans 2009), and various reporting biases, such as the notoriety bias (Pariente
85 et al. 2007). Crucially, the spontaneity of these reports often results in an incomplete recording of all
86 drugs taken by a patient. Furthermore, because the exact timing of drug administration is frequently
87 omitted, it is difficult to distinguish between simultaneous intake and medications taken at different
88 times within the same reporting window. This temporal ambiguity potentially limits the precision of
89 interaction analyses, as the observed cocktail may represent a sequence of exposures rather than
90 a concurrent pharmacological event. Consequently, because the total number of patients exposed

91 to a drug is unknown, these databases cannot provide true incidence rates, necessitating the use of
92 disproportionality analysis to identify safety signals (Almenoff et al. 2005).

93 While previous work showed that further practical experiences should be of interest for high-order
94 drug interaction testing (Tekin et al. 2018), it is hard to know which exact combination one should
95 test and easy to miss an important combination in the overwhelming space of high-order drug
96 cocktails. The present article proposes a novel method to do so. It requires the choice of a scoring
97 function able to measure, for a given AE, the importance of the disproportionality for any medication
98 set, including single medications. It then takes advantage of the tree structure of the ATC classification
99 to explore the space of medication sets in two ways: a genetic algorithm looking for the sets of high
100 score, and a MCMC algorithm learning the distribution of the scores for a given cocktail size in order
101 to evaluate how extreme a high score is. The approach is also original with respect to the fact that
102 a medication denotes either a drug or a drug family in the sense of an internal node of the ATC
103 classification.

104 The developed algorithms, available in the corresponding R package **emcAdr** (Bangard 2025), aim to
105 guide pharmacology researchers toward drug combinations that might correspond to drug interac-
106 tions and require more rigorous monitoring.

107 2 Methods

108 2.1 ATC Tree and Cocktail Definition

109 Multiple classifications of drug active ingredients exist, one being the ATC classification. This system
110 is structured hierarchically and can be represented as a tree with five levels containing, at the time,
111 6809 nodes. The leaves of this tree are the active ingredients, while the first level consists of nodes
112 representing organs or systems affected by the descendant active ingredients. The remaining nodes
113 correspond to therapeutic or pharmacological families.

114 By applying a Depth-First Search algorithm to enumerate each node of the ATC tree, we can define a
115 drug cocktail as a set of integer corresponding to specific nodes in the tree. More formally, a cocktail
116 C of size $k \geq 1$ is defined by $C = (x_1, \dots, x_k) \in \Delta^k$ where $k \in \mathbb{N}$, and Δ represents the set of numbered
117 nodes of the ATC tree T . Figure 1 shows examples in a simplified tree, the green nodes denoting the
118 considered cocktail. Note that sets of drugs of size one are also considered, and by abuse of language
119 are also referred to as cocktails.

120 Considered cocktails can include internal nodes of the tree (thus representing families of active
121 ingredients), allowing for the detection of more general signals. For example, paracetamol might
122 send a weak signal, while if we move up the tree, analgesics as a whole could represent a stronger
123 and more general signal. Therefore, all patients taking at least one drug from this drug family will
124 be considered in the computation of the risk. That notion is equivalent to the notion of cut in the
125 tree-scan method (Kulldorff, Fang, and Walsh 2003).

126 2.2 Cocktail Risk Characterization

127 In the field of pharmacology, accurately characterizing the risk associated with drug administration
128 is a complex task. The aim of the developed method is to search the space of cocktails to maximize a
129 score indicating if individuals taking a given drug combination have a higher risk of an AE. While
130 the algorithm is designed to be flexible and can be run with any scoring function, we focus on a
131 comparison of established metrics to justify our selection (see Section 3.1).

132 2.2.1 Scoring Functions in Pharmacovigilance

133 To evaluate the disproportionality of drug cocktails presence for a particular AE, several statistical
134 measures have been proposed in the literature:

135 **Proportional Reporting Ratio (RR)** A standard measure defined as the ratio of the probability
136 of an AE occurring in the group exposed to the cocktail versus the non-exposed group. Its
137 application in signal generation from spontaneous reports was notably discussed by (Evans,
138 Waller, and Davis 2001).

139 **PRR for Drug-Drug Interactions (PRR)** Unlike the single-drug PRR, this adaptation for drug
140 combinations evaluates whether a combination represents a synergistic risk. Specifically, as
141 discussed by (Wang et al. 2020), a signal is often defined by comparing the lower bound of the
142 confidence interval of the combination’s risk to the maximum risk observed for the individual
143 drug components.

144 **Ω Shrinkage** A Bayesian measure specifically developed for drug-drug-event combinations. As
145 proposed by (Norén et al. 2008), it utilizes a “shrinkage” approach to reduce false positive
146 signals in cases with limited data by pulling the observed association toward the value expected
147 under independence.

148 **Concomitant Signal Score (CSS)** Introduced as an improved detection criterion, this metric aims
149 to enhance the detection of DDI signals by building upon the PRR framework, as detailed by
150 (Noguchi et al. 2020).

151 **Proposed Score: Hypergeometric Disproportionality** While the methodology can accommo-
152 date various scores, we propose the use of a score derived from the Fisher exact test. As
153 highlighted by (Ahmed et al. 2010), this approach has the advantage of being non-asymptotic.
154 Consider a dataset of N patients, among which K experience the adverse event AE. Let n_C be the
155 number of people taking a cocktail C and x the number of patients taking C and experiencing
156 AE. We define the risk to be:

$$H(C) = -\log(\mathbb{P}(X \geq x))$$

157 where $X \sim \mathcal{H}(n_C, K, N)$ follows a hypergeometric distribution. This measure effectively functions as
158 the log p-value under the null hypothesis that the number of people with AE in a uniform sample of
159 n_C out of N people follow the hypergeometric distribution. It has the distinct advantage of accounting
160 for the total number of patients exposed to the cocktail; for instance, $H(C)$ will assign a higher risk
161 to a cocktail taken by 100 patients with 50 AE cases than to a cocktail taken by 10 patients with 5
162 AE cases, whereas simple ratios like the PRR might treat them identically. Such hypergeometric
163 measures are well-established in other high-dimensional fields like bioinformatics for functional
164 enrichment analysis (Grossmann et al. 2007).

165 2.3 Distinguishing Combined Risk from True Interaction

166 While the $H(C)$ score effectively identifies cocktails associated with a significant increase in the
167 AE frequency, it does not inherently distinguish a synergistic pharmacological interaction from
168 situations corresponding to the independent addition of individual effects or an effect driven by a
169 subset of the cocktail (e.g., “innocent” medications co-prescribed with a high-risk drug).

170 To address this, we propose a post-treatment of detected signals using Firth’s penalized likelihood
171 logistic regression (Firth 1993). This method is particularly suited for spontaneous reporting systems
172 as it reduces bias in maximum likelihood estimates and provides a solution to the problem of
173 separation, which often occurs with rare adverse events. Using the *logistf* R package (Heinze, Ploner,
174 and Dunkler 2023), we estimate a model for a given cocktail C (e.g., d_1, d_2) as follows:

$$\text{logit}(P(AE = 1)) = \beta_0 + \beta_1 \mathbb{1}_{d_1} + \beta_2 \mathbb{1}_{d_2} + \beta_3 \mathbb{1}_{d_1 \cap d_2}$$

175 An interaction is confirmed if the interaction coefficient β_3 is positive and statistically significant.
 176 This indicates that the risk associated with the co-prescription exceeds the additive effect of the
 177 individual components on the logit scale. While the emcAdr package allows the use of Firth’s
 178 penalized regression to handle the rare events and separation issues. Users may implement the
 179 post-treatment of their choice.

180 2.4 Disproportionality Identification

181 2.4.1 High-risk Drug Cocktails Identification

182 The number of possible cocktails is 2^L , where L denotes the number of nodes in the ATC tree, and
 183 even for a given cocktail size k , the number of possibilities is still $\binom{L}{k}$. It is therefore not possible to
 184 compute $H(C)$ for each possible cocktail C included in the dataset. Instead, to explore the space of
 185 cocktails and locate those at high-risk of AE, we use a genetic algorithm (Pétrowski and Ben-Hamida
 186 2017). It simulates the evolution of a population of cocktails according to the principle of natural
 187 selection, in order to search for the most performing individuals with respect to an evaluation
 188 criterion based on H .

189 The steps are the following, the algorithm repeating steps 2 and 3 until a user-defined number of
 190 iterations is reached.

191 **Initialization.** The genetic algorithm’s population consists of m cocktails. These cocktails are
 192 randomly initialized and can vary in size.

193 **Evaluation and selection.** At iteration n , the current population P_n undergoes an evaluation and
 194 selection phase. The evaluation computes the score $H(C)$ for each cocktail C in the population.
 195 A new population Q_{n+1} of the same size is drawn by sampling m times a pair of cocktails in
 196 the original population and copying the one with highest score. Note that this step performs
 197 selection as the expectation of the number of copies in Q_{n+1} of a cocktail from P_n is an
 198 increasing function of its score. A penalization is however applied to avoid a uniformisation of
 199 the population, as further explained in Section 2.4.2.

200 **Stochastic modification.** Mimicking the genetic drift in nature, stochastic modifications occur in
 201 the population in order to explore the large space of cocktails. First, a crossover operation allows
 202 two cocktails to exchange information. Here, the crossover involves exchanging sub-trees
 203 between two cocktails as follows:

- 204 • an internal node v of the ATC tree is randomly selected;
- 205 • the nodes of the subtree rooted at v are exchanged between the two sequences.

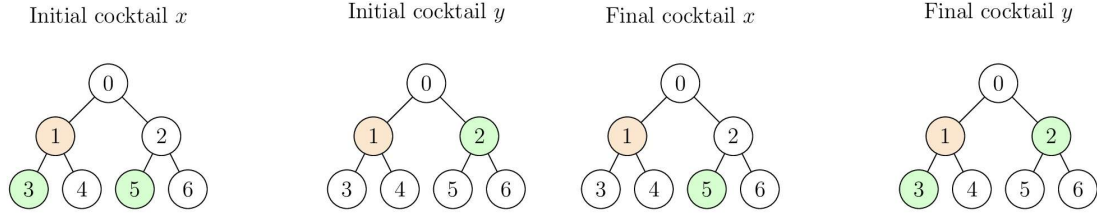
206 After performing the crossover, a mutation is applied to the resulting individuals, chosen from
 207 two types. The first type is a local mutation which changes a randomly selected node of the
 208 cocktail to one of its free neighboring nodes. This mutation is further explained in Section 2.5.
 209 The second type is an addition/deletion mutation which operates as follows, with k being the
 210 cocktail length and α a chosen hyperparameter:

- 211 • with probability $\min(1, \frac{\alpha}{k})$, a node uniformly drawn from Δ is added to the sequence;
- 212 • with probability $1 - \min(1, \frac{\alpha}{k})$, a uniformly drawn node from the cocktail is removed.

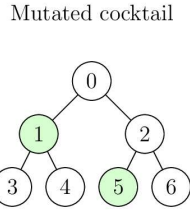
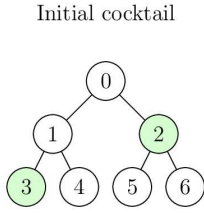
213 An example of crossover and mutations can be seen on Figure 1 (a), (c) and (d).

Applying those modifications to Q_{n+1} yields a population P_{n+1} which is used to loop at step 2.

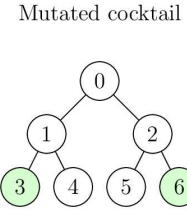
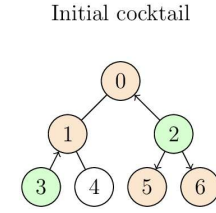
(a) Crossover



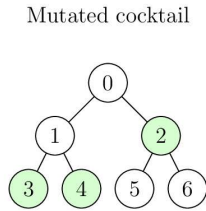
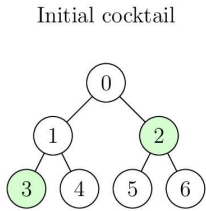
(b) Random mutation



(c) Local mutation



(d₁) Addition



(d₂) Deletion

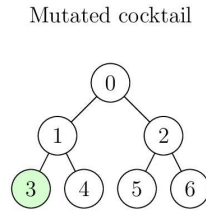
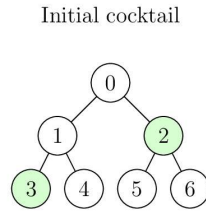


Figure 1: Cocktail modifications used for the genetic algorithm (a, c and d) and the MCMC algorithm (b and c). Green nodes are part of considered cocktails. In Crossover, the orange node represents the selected internal node whose subtrees are being swapped. In local mutations, orange nodes represent legal moves

2.4.2 Distance between drug cocktails and cocktail penalisation

If at some point of the algorithm, an individual of P_n has a high score compared to other individuals, the genetic algorithm may converge to a population consisting entirely of that cocktail. To avoid this uniformisation phenomenon, similar cocktails are penalized in the evaluation phase as follows,

$$H_{pen}(C) = \frac{H(C)}{\sum_{C_i \in \mathcal{C}} \text{Sim}(C, C_i)}$$

The computation of the similarity $\text{Sim}(C, C')$ is based on a distance inspired by the Levenshtein distance (Levenshtein et al. 1966). However, unlike the traditional Levenshtein distance, sequences are treated as unordered sets. For two drug cocktails, C_1 and C_2 , of sizes n_1 and n_2 , the distance $d(C_1, C_2)$ is defined as the minimal cost required to transform C_1 into C_2 using three elementary operations.

- $\text{Ins}_a(C)$ consists of adding a to the cocktail C .
- $\text{Del}_a(C)$ consists of deleting a from the cocktail C .
- $\text{Sub}_{a,b}(C)$ consists of substituting $a \in C$ by b .

An associated cost is defined for each operation.

228 **Substitution.** The cost associated with the substitution operation is chosen to be consistent with
 229 the conceptual similarity of cocktails. If a is a drug belonging to C , the cost should increase as
 230 the drug b diverges further from drug a . For example, if a is a drug, and b a drug family that
 231 contains a , the cost should be moderate. Conversely, if b is a drug family not containing a the
 232 cost should be higher. This distance is thus defined by the maximal distance between a and b
 233 to their Lowest Common Ancestor.

234 **Insertion, Deletion.** The deletion and insertion cost are chosen as $\frac{\text{depth}(T)}{2}$. This choice implies
 235 that a substitution always costs less than a deletion followed by an insertion. The latter are
 236 used only when the two cocktails do not have the same length.

237 A transformation f from C_1 to C_2 is a composition of elementary operations that go from C_1 to C_2 .
 238 The associated cost $\text{cost}(f)$ is defined as the sum of the cost of the operations used in f . Finally,
 239 $d(C_1, C_2) = \min_f \text{cost}(f : f(C_1) = C_2)$.

240 Finally, the maximum distance between C_1 and C_2 being $(n_1 + n_2)\frac{\text{depth}(T)}{2}$, we define the similarity as

$$\text{Sim}(C_1, C_2) = 1 - \frac{2D(C_1, C_2)}{(n_1 + n_2)\text{depth}(T)}$$

241 The computation of the similarity is achievable in $\mathcal{O}(n_1 \times n_2 \times \text{depth}(T) + |\Delta|)$ operations in the worst
 242 case. The algorithm to compute the similarity is detailed in the Section 5.1 (see Algorithm 1).

243 2.4.3 Output clustering

244 Despite the diversity mechanisms integrated into the genetic algorithm, not all drug cocktails
 245 retrieved within the genetic algorithm population are unique. It is moreover common to encounter
 246 solutions that are merely variations of others, differing only by transformations such as changing
 247 a node in the ATC tree to its parent or child. To streamline analysis and enhance the efficiency, a
 248 post-treatment clustering of similar drug cocktails is implemented. This method allows to focus on
 249 the most risky cocktails within each cluster or to interpret pharmaceutically clusters rather than
 250 individual cocktails.

251 To do so, drug cocktails are embedded into a two-dimensional space using the UMAP algorithm
 252 (McInnes, Healy, and Melville 2018), which aims to preserve similarity in the latent space. This
 253 representation enables the effective use of conventional machine learning clustering algorithms in
 254 \mathbb{R}^2 . Specifically, the DBSCAN algorithm (Ester et al. 1996) is applied to identify clusters of similar
 255 drug cocktails with an intuitive way of choosing hyperparameters.

256 2.5 Approximate P-Value Assignment for Drug Cocktails

257 Once a list of cocktails of high score has been established by the genetic algorithm, an important
 258 step of the analysis is to assign them p-values to decide if they are significant.

259 Consider a cocktail C of size k in the list and its score S_{obs} . Denote by H_0 the null hypothesis according
 260 to which a cocktail does not favor the AE, and by N_0 the number of cocktails of size k for which H_0
 261 is the truth. Similarly, H_1 represents the alternative hypothesis of a cocktail favoring the AE and N_1
 262 is the number of such cocktails of size k . The p-value corresponding to S_{obs} is then $\mathbb{P}_{H_0}(S > S_{obs})$, but
 263 cannot be estimated without modelisation hypothesis under H_0 .

264 However, if $\mathbb{P}_M(S)$ refers to the marginal distribution, that is the score distribution for the cocktails
 265 both in H_0 and H_1 ,

$$\mathbb{P}_M(S > S_{obs}) = \mathbb{P}_{H_0}(S > S_{obs}) \frac{N_0}{N_0 + N_1} + \mathbb{P}_{H_1}(S > S_{obs}) \frac{N_1}{N_0 + N_1}$$

266 so that

$$\frac{N_0 + N_1}{N_0} \mathbb{P}_M(S > S_{obs}) - \frac{N_1}{N_0} \mathbb{P}_{H_1}(S > S_{obs}) \leq \mathbb{P}_{H_0}(S > S_{obs}) \leq \frac{N_0 + N_1}{N_0} \mathbb{P}_M(S > S_{obs})$$

267 Under the reasonable assumption $N_1 \ll N_0$, the probability $\mathbb{P}_M(S > S_{obs})$ on the marginal distribution
 268 can thus be used as an approximation of the p-value. Note that the upper bound yields that, under
 269 the weak hypothesis that less than 10% of the cocktails of size k favor the AE, the real p-value is at
 270 most equal to 1.11 times its approximation. Moreover, the approximated p-value can be estimated by
 271 computing the score of cocktails sampled in the general cocktail population. The proposed method
 272 therefore focuses on a sampling scheme in the general population and uses the approximated p-value
 273 to declare significance.

274 A naive sampling of cocktails considers almost only cocktails taken by no patient in the dataset. A
 275 Metropolis-Hastings MCMC algorithm is thus considered, as it can be used by conditioning on the
 276 fact that all visited cocktails are present in the dataset (Au and Beck 2001).

277 To employ such an algorithm, it is necessary to define a state space $\mathcal{C} = \{C_1, \dots, C_p\}$, a computable
 278 target measure $f(C_i)$, and conditional laws $q(\cdot|C_i)$ under which simulation is possible and new states
 279 can be proposed.

280 **State set.** The state set is made of all cocktails of k drugs for a fixed k .

281 **Proposal law.** The proposal law is defined as a mixture of two mutation laws of the current cocktail.
 282 They operate as follows:

- 283 • Random mutation consists of a completely random movement in the cocktail space.
- 284 • Local mutation involves a local movement relative to the structure of the drug tree. Here,
 285 a node x_p of the state C_i is changed to one of its free neighboring nodes.

286 At each iteration, the random and local mutations have probability p_R and $1 - p_R$, where p_R is a
 287 hyperparameter.

288 Figure 1 (b, c) presents examples of a random and a local mutations.

289 **State evaluation.** The evaluation of a drug cocktail is based on the score $H(C)$. The chosen target
 290 measure is then:

$$f_T(C_i) = \frac{1}{Z(T)} \times e^{\frac{H(C_i)}{T}}$$

291 where $Z(T) = \sum_C e^{\frac{H(C)}{T}}$. T is a parameter known as temperature, which modulates space
 292 exploration by more readily accepting cocktails with moderate scores (high T) or, conversely,
 293 by strongly favoring combinations of drugs with high scores (low T).

294 The acceptance probability of cocktail C_{i+1} from cocktail C_i is given by:

$$\min\left(1, \frac{f_T(C_{i+1})}{f_T(C_i)} \times \frac{q(C_i|C_{i+1})}{q(C_{i+1}|C_i)}\right)$$

295 The theory related to the Metropolis-Hastings algorithm (Robert and Casella 2004) ensures that
 296 the empirical distribution of $f_T(C_i)$ for the constructed cocktail chain converges to the distribution

297 of $f_T(C)$. A very long realization of such a walk, therefore, allows for the approximation of the
298 distribution that can be used to determine an empirical p-value for the score of a cocktail of interest.
299 This enable the possibility to say whether or not a high-risk is truly significant (e.g. among the top
300 5% of scores). It defines what a high risk is in our case.

301 2.6 Datasets

302 2.6.1 Simulated data

303 Multiple datasets were simulated to evaluate the method performance against known outcomes. The
304 datasets, designed to challenge the algorithm, simulate various patient scenarios. Each patient record
305 includes prescribed medications and the corresponding occurrence of an adverse event *AE*.

306 The first dataset is composed of 200,000 patients, and has the following characteristics:

- 307 • 1% of the patients take a size-3 drug cocktail C_1 and have a $\frac{1}{100}$ chance of having *AE*.
- 308 • 1% take a size-3 drug cocktail C_2 and have a $\frac{1}{200}$ chance of having *AE*.
- 309 • 1% take a size-2 drug cocktail C_3 and have a $\frac{1}{100}$ chance of having *AE*.
- 310 • 1% take a size-2 drug cocktail C_4 and have a $\frac{1}{200}$ chance of having *AE*.

311 A small percentage of the dataset (1.5% per combination) are combinations of 2 out of the 3 drugs
312 from C_1 and C_2 , but with no risk of *AE*. This helps to mitigate the false identification of sub-cocktails
313 of C_1 and C_2 as high risk cocktail because those who take two drugs of these cocktails will almost
314 surely take the remaining drug of the cocktail.

315 The remaining 87% of the datasets consists of patients assigned with random cocktails drawn
316 uniformly. The size s of each cocktail is drawn according to a Poisson distribution with $\lambda = 4$ (mean
317 size of drugs cocktail taken by patients in the dataset). For each cocktail, s nodes of the ATC tree are
318 selected uniformly, with each combination assigned an adverse event with probability $\frac{1}{15000}$.

319 Three others datasets were similarly constructed, the difference lying in the size of the cocktails
320 inducing *AE*. One has only size-two cocktails, other only size-three cocktails and the last one,
321 size-two, three and four cocktails.

322 2.6.2 FAERS Data

323 As a proof-of-concept on real data, the method was also assessed using the FAERS dataset, which
324 consists of ICSRs submitted by healthcare professionals, consumers, and manufacturers. These
325 reports include details on patient drug intake and the side effects experienced. The methods were
326 deployed our on FAERS data from the second quarter of 2013 to the second quarter of 2015, the
327 restriction to a two-year window corresponding to the will of limiting computational time.

328 Significant refinement of the FAERS data was required. Duplicate reports were removed, retaining
329 only the report with the most recent ID. Subsequently, a link was established between the prescribed
330 drugs and the ATC codes of each active ingredient. This process involved matching drug names to
331 their respective active ingredients and converting these ingredients to their corresponding ATC codes.
332 The DiANA dictionary (Fusaroli et al. 2024) facilitated the standardization of FAERS drug names
333 to ATC codes. It is important to note that the DiAna dictionary handles combination products by
334 splitting them into their constituent active substances rather than assigning a single ATC combination
335 code. Reports with unmatchable drug names in the DiANA dictionary were excluded, reducing the
336 dataset from 2,043,231 to 1,612,931 patients.

337 For this study, we focused on myopathy as the selected adverse event outcome. It is a clinically
338 concerning condition with a sufficient number of reported cases in the dataset (536 cases). To validate

our results, we compared the identified drug-myopathy associations with known drugs already established to cause myopathy Valiyil and Christopher-Stine (2010). Code for data refinement is available on [GitHub](#).

3 Results

3.1 Score Comparison

To support the use of the hypergeometric score $H(C)$ introduced in Section 2.2, we compared it to other risk scores on simulated data. The simulated dataset comprises pairwise drug combinations. A subset of these cocktails was generated under the alternative hypothesis H_1 , meaning they are specifically associated with an increased probability of the AE (see Section 2.6.1). The remaining cocktails were sampled under the null hypothesis H_0 , representing a baseline risk without specific interaction. Figure 2 illustrates the performance of the risk scoring methods for detecting high-risk drug combinations introduced in Section 2.2.1. Each subplot displays the score values for cocktails representing true solutions, sampled under H_1 (green) and cocktails not representing true solutions, sampled under H_0 (red). The bottom-right panel presents the Precision-Recall (PR) curve, comparing the detection power of the scores in identifying high-risk cocktails. PRR is a special score because its value is either one or zero, which allows the computation of only one value of precision and recall. PRR is therefore represented by a single point rather than a PR curve.

PR curves of the different scoring methods are mainly comparable, confirming the conclusions of (Candore et al. 2015). However, as illustrated by the jitter plots, the hypergeometric score and the Ω Shrinkage measure better rank and isolate true solutions from other cocktails. It must be emphasized that the Ω Shrinkage measure is difficult to compare using a threshold, as the original article (Norén et al. 2008) suggests signaling a cocktail when the score exceeds zero. However, in the simulations, the computed score never exceeded zero, as depicted by the x-axis of its jitter plot. Despite these considerations, these two methods are the least biased toward cocktails taken by only a few patients.

The good behavior of the hypergeometric score and its easy generalisation to cocktails of any size justify the use of that scoring function for the exploration of the cocktail space.

3.2 Application to the Simulated Dataset

3.2.1 Estimation of Risk Distribution

Risk distribution was estimated for size-two drug cocktails on Section 2.6.1 dataset. Estimation of risk distribution for higher cocktails sizes are possible but it is nearly impossible to compare it to the true distribution as it is computationally prohibitive to obtain. The distribution estimated by the MCMC algorithm, is compared to the true risk distributions in Figure 3.

The left panels display the distributions of risk scores for both the estimated (top-left) and true (bottom-left) risk values. Both distributions share a similar shape, with the majority of risk scores concentrated at low values, as 95% of the scores fall below 11. However, some differences can be observed, particularly in the tail of the distribution, where cocktails of higher risks are under-represented in the estimated distribution.

The right panel of Figure 3 presents a Probability-Probability (PP) plot (top) and a Quantile-Quantile (QQ) plot (bottom), comparing the quantiles and probabilities of the estimated and true risk distributions. While the right panel of the figure demonstrates good agreement at lower risks, where most of the data lie, deviations at higher risk values suggest that the estimated distribution slightly underrepresents the risk for more extreme values.

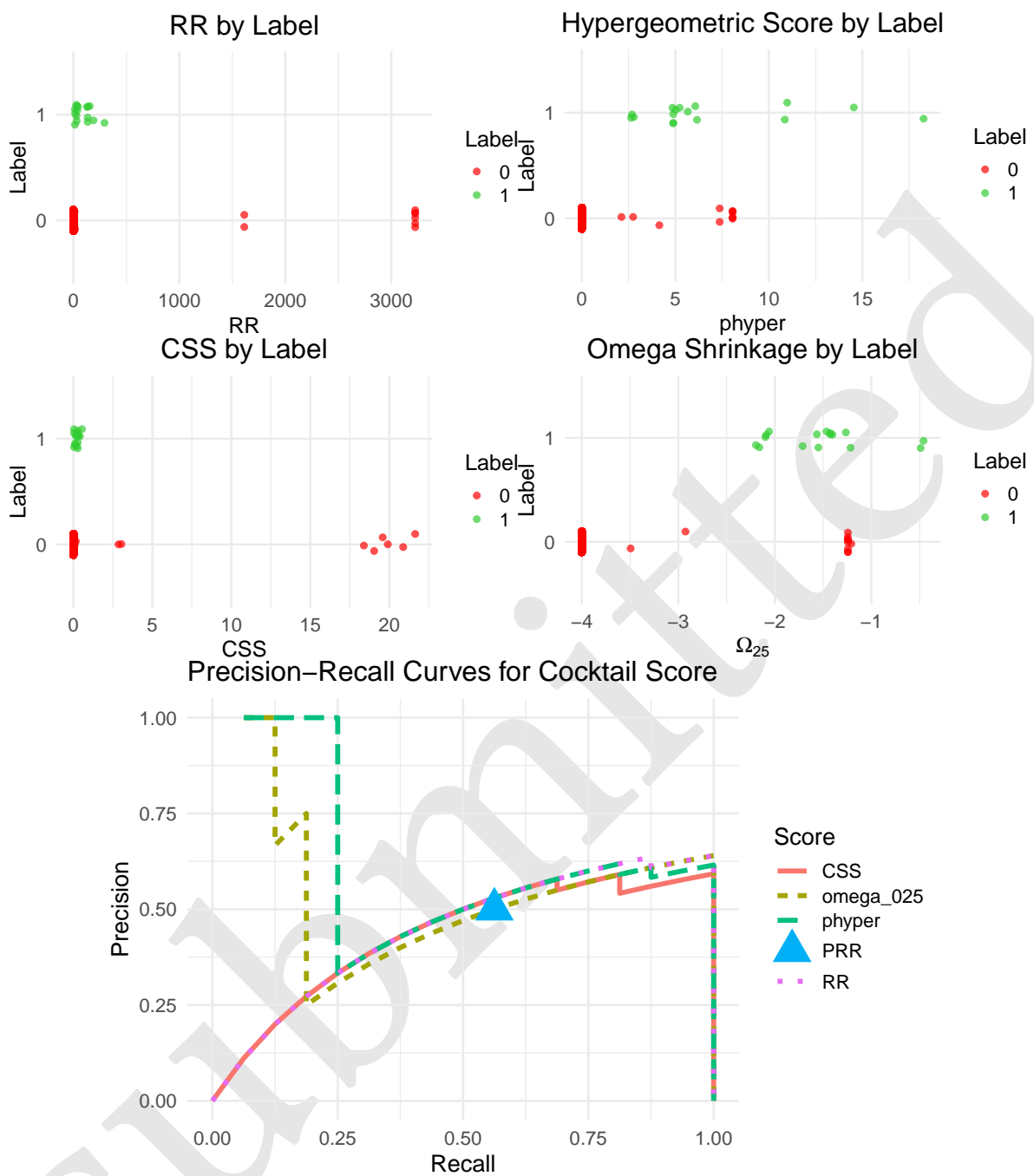


Figure 2: Comparison of scores for cocktail of size-two. Each dots denotes a cocktail while his risk computed on the formerly presented synthetic dataset (Section 2.6.1) is showed on the x-axis. Red dots represent cocktails that do not induce adverse event (negative controls), green ones represent cocktail inducing adverse event (positive controls). The bottom-right corner shows the Precision-Recall curves for each score. The perfect classification corresponds to the upper right corner. The areas under the curves allow to compare different methods. RR, PRR, Omega shrinkage, phyper and the CSS are defined in Section 2.2.1.

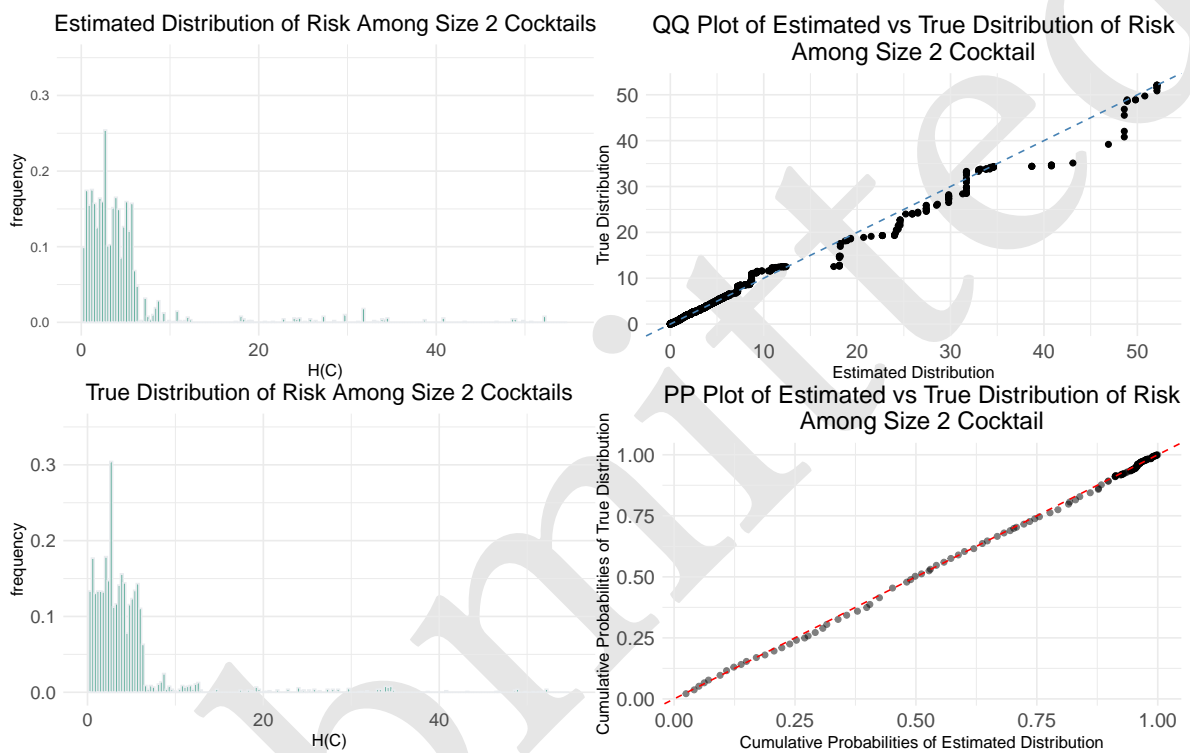


Figure 3: Comparison of estimated and true risk distributions for size-two drug cocktails. Left panels show comparison of risk distribution among size-two cocktails, right panels allows to compare probabilities and quantiles of both distributions

381 Results indicate that the method performs well in estimating risk scores for the majority of cocktails,
382 capturing the overall risk distribution with reasonable accuracy. The slight underestimations which
383 are present for high-risk cocktails are not a problem since the interest of the method is to assign
384 p-values. P-values are still reliable as shown in the PP-plot, Figure 3. Consequently, we can assign
385 robust empirical p-values to any size-two cocktails based on their risks. Furthermore the calibration
386 under the null hypothesis for the p-values attributed by the algorithm is assessed in Section 5.2.

387 3.2.2 Genetic algorithm output and clustering

388 The genetic algorithm was applied to the simulated dataset to identify high-risk drug cocktails.
389 Multiple runs of the algorithm were conducted using different hyperparameter sets (population size,
390 number of generations, parameter α) to ensure the visit of different regions of the space of possible
391 cocktails. The results were subsequently concatenated to create a comprehensive list of high-risk
392 cocktails.

393 The genetic algorithm successfully identified nearly all high-risk size-two and size-three drug cocktails
394 in the simulated dataset (Figure 4). For size-two cocktails, the algorithm consistently found the
395 exact high-risk combinations. However, for size-three cocktails, the algorithm sometimes identified
396 cocktails that were very close to the true high-risk combinations, missing only one drug from the
397 correct cocktail in a few cases (oftentimes, choosing parent nodes instead of the actual drugs).

398 To streamline the analysis of the large set of results, significant cocktails were filtered using the
399 empirical p-value by setting a threshold of 5%. Clustering techniques were then applied to group
400 similar cocktails together. As discussed in Section 2.4.3, the UMAP algorithm has been used for
401 dimensionality reduction, followed by the DBSCAN clustering method. This post-processing step
402 allows to reduce redundancy by grouping cocktails that differed only slightly, such as by substituting
403 a drug for another within the same pharmacological family. Such cocktail would have similar medical
404 interpretations.

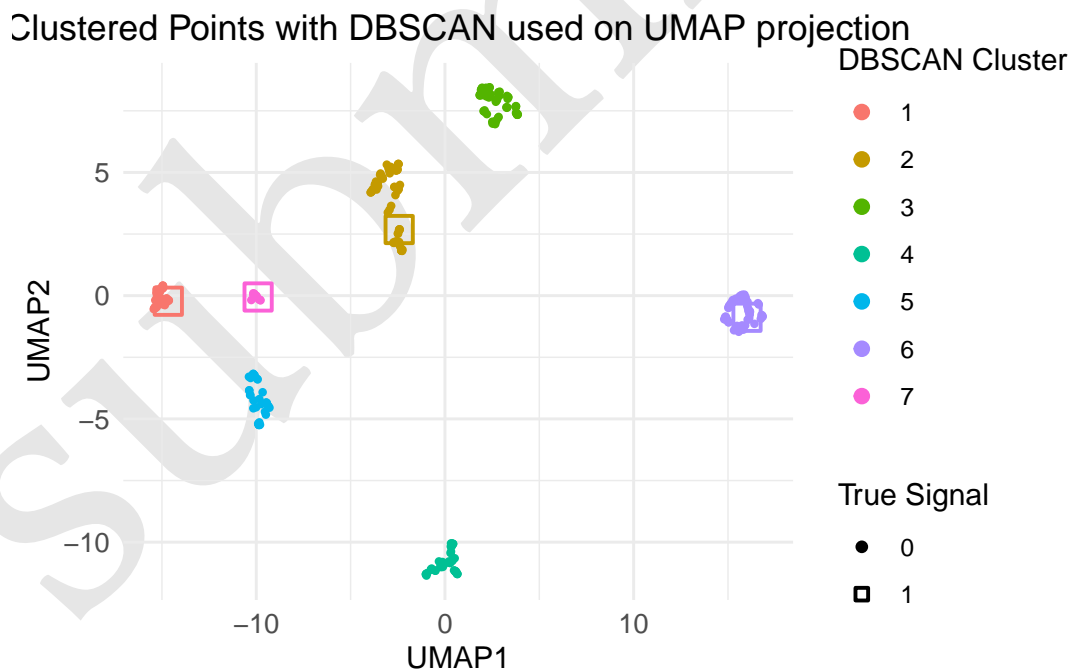


Figure 4: Clustering of high-risk drug cocktails identified by the genetic algorithm on the simulated dataset. Each dot represents a drug cocktail, true cocktail solutions are the centers of the squares

405 Figure 4 illustrates the results of the clustering process after mapping the selected cocktails in

406 the plane. Each point represents a drug cocktail, and the 7 automatically determined clusters are
407 represented by the colors.

408 The first conclusion is that the clusters are well separated in terms of the editing distance defined
409 in Section 2.4.2. The genetic algorithm thus identified seven regions of the cocktails space of high
410 score that are different in terms of interpretation as their cocktails are far away between classes.
411 On the other hand, cocktails in the same clusters are close, indicating a possible pharmacological
412 interpretation of the cluster.

413 The second conclusion is that the algorithm effectively found the true solutions or at least very similar
414 solutions. Indeed, the embedding of the true solutions yields the four squares, that clearly belong
415 to four different clusters among the seven. The method therefore identifies and separates regions
416 of the cocktail space containing the true solutions. That simulation thus enhances the confidence
417 that investigating the high-score cocktails returned by the methods may allow to detect relevant
418 phenomena.

419 **3.3 Application to the FAERS Spontaneous Reporting Data**

420 **3.3.1 Estimation of Risk Distribution**

421 The risk estimation method was applied to the FAERS spontaneous reporting dataset presented in
422 Section 2.6.2. Figure 5 presents a comparison between the estimated risk distribution and the true
423 risk distribution for size-two drug cocktails. The left panel of the figure shows the distributions of
424 risk scores, while the right panel presents the QQ plot and the PP plot, comparing the quantiles and
425 probabilities of both distributions.

426 The histogram reveals that the estimated distribution aligns well with the true distribution for the
427 majority of cocktails with lower risk scores. However, deviations begin to emerge in the tail of the
428 distribution. Specifically, 15 of the riskiest cocktails in the true distribution were not captured by
429 the estimated distribution as we see in the QQ plot. This explains the observed shift in the QQ plot
430 at the highest quantiles since higher risk cocktails have not been found by the MCMC algorithm,
431 highlighting the need of a complementary method like the genetic algorithm in order to find riskiest
432 cocktails.

433 Despite this slight deviation, the empirical p-values remain robust for both lower and higher-risk
434 cocktails as shown by the PP-plot in the Figure 5.

435 **3.3.2 Genetic algorithm output and clustering**

436 The genetic algorithm was applied on the FAERS data focusing on the myopathy AE by running 180
437 parallel executions of the genetic algorithm on varying population sizes (from 100 to 1000 cocktails
438 per generation). The whole procedure run in less than 8 hours on a 24-core server.

439 Cocktail sizes present in the merged final populations vary from 1 to 6. The MCMC algorithm was
440 run for each cocktail size in this range to assign an empirical p-value to each solution. All solutions
441 having a p-value lower than 0.05 were kept. No multiple testing correction was made in order to
442 avoid false negatives, that is disregarding interesting cocktails, even if this may inflate the number of
443 false positives. 682 drug cocktails composes the final list. Applying Benjamini-Hochberg corrections
444 to control the FDR at level 5% and 10% respectively kept the first 107 and 564 elements of the list.

445 The clustering procedure was applied to the 682 cocktails, leading to 15 clusters. To validate the
446 results, the first 150 solutions were tagged with the families they correspond to, if any, without
447 knowledge of the clustering's result. To do so, some drugs or drug families known to be linked to
448 myopathy adverse events were considered, that is hypolipemic drugs, Colchicine, corticosteroids,

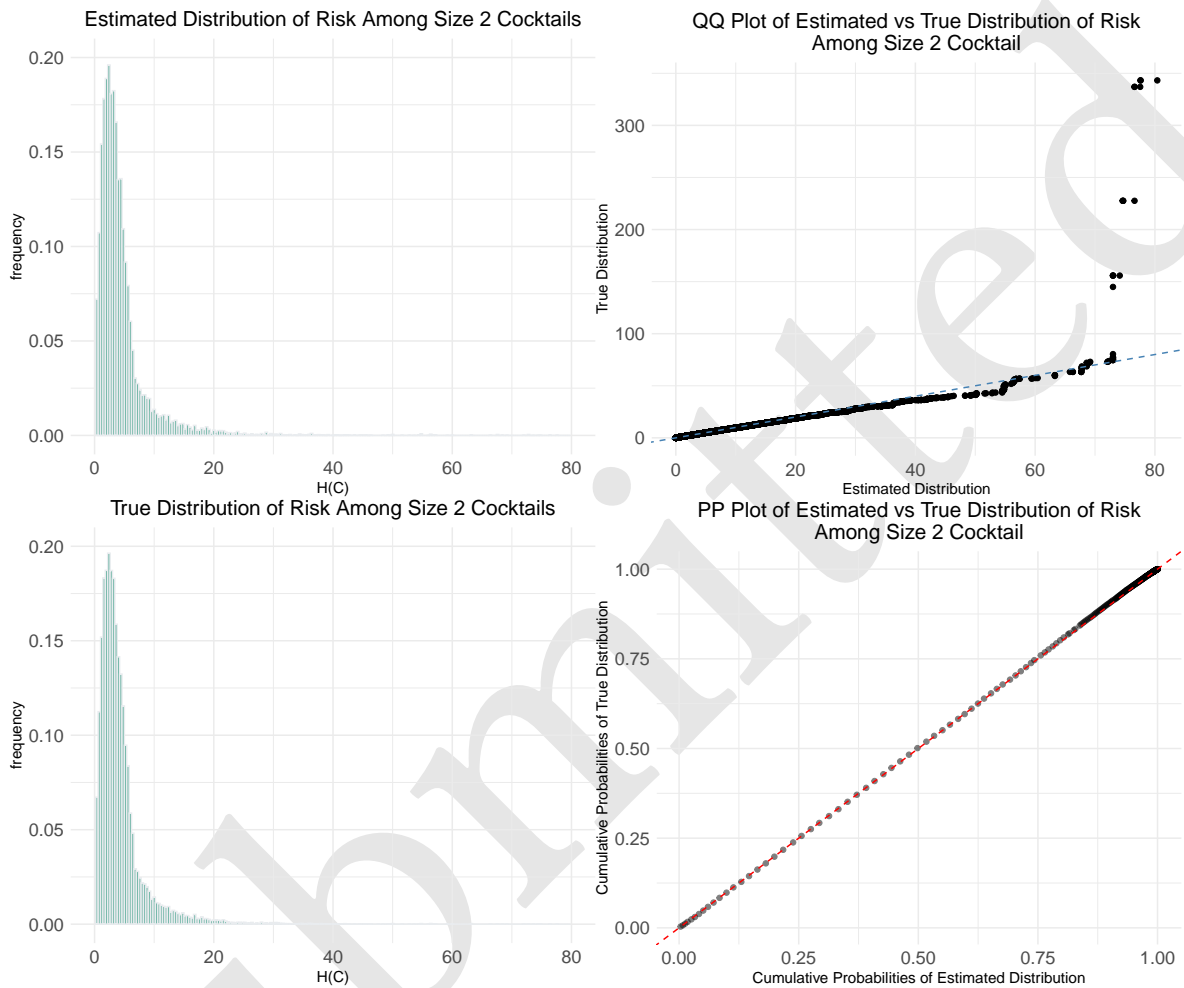


Figure 5: Comparison of estimated and true risk distributions for size-two drug cocktails on the FAERS dataset presented Section 2.6. Left panels show comparison of risk distribution among size-two cocktails, right panels allows to compare probabilities and quantiles of both distributions. Left distributions are truncated to 80 for visualization purposes. A few cocktails have a risk around 300 as shown on the Y-axis of the QQ plot.

449 Ciclosporine, Beta blocking agents, Fluoroquinolones, and anti-malaria drugs (Miernik, Matusiewicz,
450 and Olesińska 2024; Hall, Finnoff, and Smith 2011; Valiyil and Christopher-Stine 2010).

451 The final result is a table of 682 rows, one per selected cocktail, indicating its composition, the number
452 of patients taking it, the number of patient taking it and facing myopathy, hypergeometric and RR
453 score. It also contains the cluster it belongs to and the tagged families. The entire table is available
454 [on this link](#). Table 1 summarizes the cluster assignments for the top 150 cocktails identified in the
455 genetic algorithm. Among these, eleven cocktails could not be assigned to any drug or drug family
456 listed in the table headers. Note that a cocktail can be associated with more than one drug or drug
457 family.

Table 1: Summary of clustering applied to the identified solutions. Each row corresponds to a cluster. The 150 cocktails with the highest risk were analyzed. Box (i, j) in the table represents the number of cocktails in cluster i that include the drug or drug family j

Cluster	Hy- polipemic Drugs	Colchicine	Steroids	Cy- closporine	Beta blocking agents	Domperi- done	Fluoro- quinolones
1	31	0	3	0	0	0	4
2	0	11	0	4	0	0	0
3	7	0	0	0	19	0	0
4	0	0	0	0	0	50	0
5	0	0	0	0	0	19	0
6	0	0	0	0	0	0	4

458 This table shows the method’s capability to detect known ADRs from the FAERS dataset and highlights
459 the ability of the clustering method to group cocktails with similar pharmacological interpretations.
460 Specifically, cluster 1 corresponds to cocktails containing Hypolipemic Drugs, cluster 2 to Colchicine
461 and Cyclosporine, cluster 3 to beta blocking agents and cluster 6 to Fluoroquinolones. These clusters
462 align with previously reported pharmacological associations (Miernik, Matusiewicz, and Olesińska
463 2024). Similarly, clusters 4 and 5 correspond to Domperidone-containing cocktails which have
464 been associated with adverse effects, including potential cardiac complications, as reported by the
465 British Medicines and Healthcare products Regulatory Agency (Medicines and Healthcare products
466 Regulatory Agency 2014).

467 Interestingly, additional drug families reported in (Miernik, Matusiewicz, and Olesińska 2024), such
468 as anti-malarial drugs, were also identified but at later ranks. For instance, anti-malarial drugs are
469 primarily grouped in cluster 9, as shown in the complete solution table.

470 4 Conclusion

471 As co-medication becomes increasingly common, there is a growing need for methods capable
472 of detecting signals of harmful drug combinations from the available large databases for further
473 assessment. The proposed method addresses this need by identifying signals and assigning them
474 a p-value using a hypergeometric disproportionality analysis measure. Additionally, the method
475 enables the identification of broader signals within the ATC hierarchy by proposing “cocktails” of
476 not only active substances but also chemical, therapeutic, and anatomical families, leveraging the
477 hierarchical classification of active substances.

478 Application on synthetic datasets demonstrated that using the hypergeometric score reduces the
479 false positives from cocktails taken by a small number of patients, enhancing the robustness of

480 the measure. The results on these datasets of our MCMC algorithm to estimate the distributions
481 of cocktail risks were encouraging, as the estimated distributions closely aligned with the true
482 distributions, indicating reliable p-value assignment. Furthermore, the genetic algorithm effectively
483 identified the majority of the harmful cocktails, with a high success rate, highlighting its efficiency
484 in navigating the large solution space.

485 Applying this method to previous FAERS data for the myopathy adverse event yielded promising
486 results. A literature review confirmed the intersection between the identified signals and drugs known
487 to have a higher likelihood of causing myopathy, demonstrating the effectiveness of the proposed
488 methodology. Results also indicate that certain drug combinations are more strongly associated with
489 myopathy than individual medications. Notably, the cyclosporine/colchicine combination exhibits a
490 higher hypergeometric score (73.1 vs. 63.4) and PRR (879.4 vs. 57.1) compared to colchicine alone,
491 reinforcing the importance of analyzing drug interactions in pharmacovigilance. This combination
492 is known to be more likely to induce myopathy (Ducloux et al. 1997).

493 Furthermore, our approach identified a size-four drug cocktail (metformin, prasugrel, bisoprolol,
494 simvastatin) associated with an increased risk signal (hypergeometric score = 72.2, RR = 3060.6). This
495 combination was observed in nine patients, all of whom experienced the adverse event. While this
496 finding demonstrates the feasibility of detecting higher-order drug interactions, we emphasize that
497 no clinical validation is currently available for this specific combination. This underscores both the
498 potential of the method in identifying complex drug interactions and the need for further validation
499 through complementary studies.

500 The application of the post-treatment logistic regression to the strongest signals provided further
501 clinical refinement. For instance, the interaction between cyclosporine and colchicine was confirmed
502 as an additional interaction effect: even after accounting for individual drug effects, the coefficient
503 associated with the combined cocktail remained positive and highly significant ($p = 1.02e^{-6}$). This
504 result corroborates existing medical literature indicating a potentiation of muscle toxicity.

505 Conversely, the analysis of the identified size-four cocktail (metformin, prasugrel, bisoprolol, sim-
506 vastatin) revealed that the risk signal was almost entirely explained by a size-three sub-cocktail
507 (metformin, bisoprolol, simvastatin). In this instance, the addition of the fourth medication did
508 not yield a significant additional interaction effect. This finding highlights the importance of the
509 post-treatment step in identifying the “core” of an interaction.

510 This approach can also be extended to other settings where adverse events are explored. For instance,
511 the method could be applied using the ICD diagnosis classification or the MedDRA system, both
512 of which are hierarchical classifications. Such an application would facilitate the identification of
513 symptoms associated with the consumption of drug combinations.

514 The proposed method is implemented as an R package *emcAdr*, available on GitHub and on the
515 CRAN (Bangard 2025). A tool allowing the process of quarterly FAERS xml files to csv file directly
516 usable by our method is also available on [Github](#).

517 For researchers and stakeholders it is crucial to remember that our method is hypothesis generating
518 as are other signal detection methods in single medications. These methods aim to generate as
519 few false negative results as possible but with the trade-off of more false positives. This means
520 that any results should firstly be assessed for biological plausibility as well as validated in a more
521 formal causal framework such as RCTs and target trial emulations. Furthermore, while spontaneous
522 reporting systems have a key role in pharmacovigilance, they have known drawbacks as underlined
523 in the introduction. They however provide important knowledge about the safety of drugs, and with
524 our method also drug cocktails.

525 Funding

526 This work was partially supported by the “PHC AURORA” programme (project number: 49704QC),
527 funded by the French Ministry for Europe and Foreign Affairs, the French Ministry for Higher
528 Education and Research and the Norwegian Council for Research.

529 5 Appendices

530 5.1 Appendix A : Distance Pseudo-code Algorithm

Algorithm 1 CalculateDistance

Require: Matrix M , Lists $idxC_1$, $idxC_2$

Ensure: Cost of the distance calculation

```
1:  $height \leftarrow 0$ 
2:  $cost \leftarrow 0$ 
3: while  $idxC_1 \neq \emptyset$  and  $idxC_2 \neq \emptyset$  do
4:   for all  $iC_1 \in idxC_1$  do
5:     for all  $iC_2 \in idxC_2$  do
6:       if  $M[iC_1][height] = M[iC_2][height]$  then
7:          $cost \leftarrow cost + height - \min(M[iC_1].count(M[iC_1][0]), M[iC_2].count(M[iC_2][0])) + 1$ 
8:         remove  $iC_1$  from  $idxC_1$ 
9:         remove  $iC_2$  from  $idxC_2$ 
10:        break
11:      end if
12:    end for
13:  end for
14:   $height \leftarrow height + 1$ 
15: end while
16:  $insertion\_cost \leftarrow ATC\_HEIGHT / 2$ 
17:  $cost \leftarrow cost + (|idxC_1| + |idxC_2|) \times insertion\_cost$ 
18: return  $cost$ 
```

531 Algorithm 1 computes the distance between two cocktails, C_1 and C_2 , based on three inputs.

532 The first input is an integer matrix M . This matrix represents the nodes of C_1 and C_2 , as well as
533 their corresponding parent nodes. The matrix has dimensions (PN, ATC_HEIGHT) , where P and N
534 denote the sizes of C_1 and C_2 , respectively. For example, consider the simplified tree shown in Figure
535 1 of the article. In this tree, C_1 could be the cocktail containing only the node [3], and C_2 could be
536 the cocktail containing only the node [2] ($P = 1$ and $N = 1$).

537 The corresponding matrix M would be:

$$M = \begin{bmatrix} 3 & 1 & 0 \\ 2 & 2 & 0 \end{bmatrix}$$

538 The second input consists of $idxC_1$ and $idxC_2$, which represent the indices of the rows in M that
539 contain the nodes of C_1 and C_2 , respectively.

5.2 Appendix B : Calibration Under the Null

To assess the validity of the approximation of the p-value, we plotted the empirical distribution of p-values for cocktails presumed not to increase the adverse-event rate on the synthetic dataset. The theoretical p-values following a Uniform(0, 1) distribution, the approximated ones should exhibit a distribution close to uniform if the approximation is valid. Figure 6 shows a histogram of these p-values, which appears approximately flat.

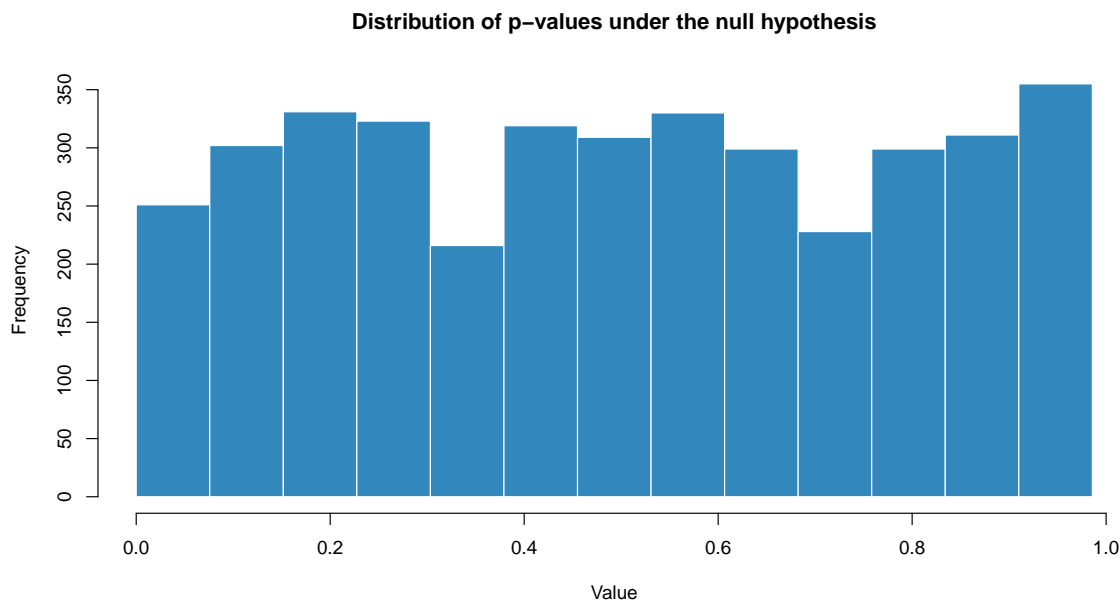


Figure 6: Histogram of p-values for cocktails presumed to satisfy the null hypothesis on synthetic dataset (no elevated adverse-event risk)

5.3 Appendix C : FAERS Clustering

Figure 7 shows the clustering applied to the results of the genetic algorithm ran on the FAERS datasets.

5.4 Appendix D : Algorithmic Complexity

The total time complexity of the high-risk cocktail identification is given by:

$$\mathcal{O}(G \cdot P \cdot T_{eval})$$

Where G represents the number of generations (or MCMC iterations) and P represents the population size of the GA (this equals one for the MCMC algorithm). The evaluation time for a single cocktail, T_{eval} , is defined by the matching logic required to count occurrences across the database:

$$T_{eval} = \mathcal{O}(N \cdot K \cdot R)$$

- N (Number of Reports): The algorithm iterates once through the database to compute the hypergeometric score for a given cocktail. The runtime scales linearly with the number of patients.
- K (Cocktail Size): The number of drugs in the candidate cocktail. In this study, K is typically small since there is a limit of drug a patient take.

Clustered Points with DBSCAN used on UMAP projection

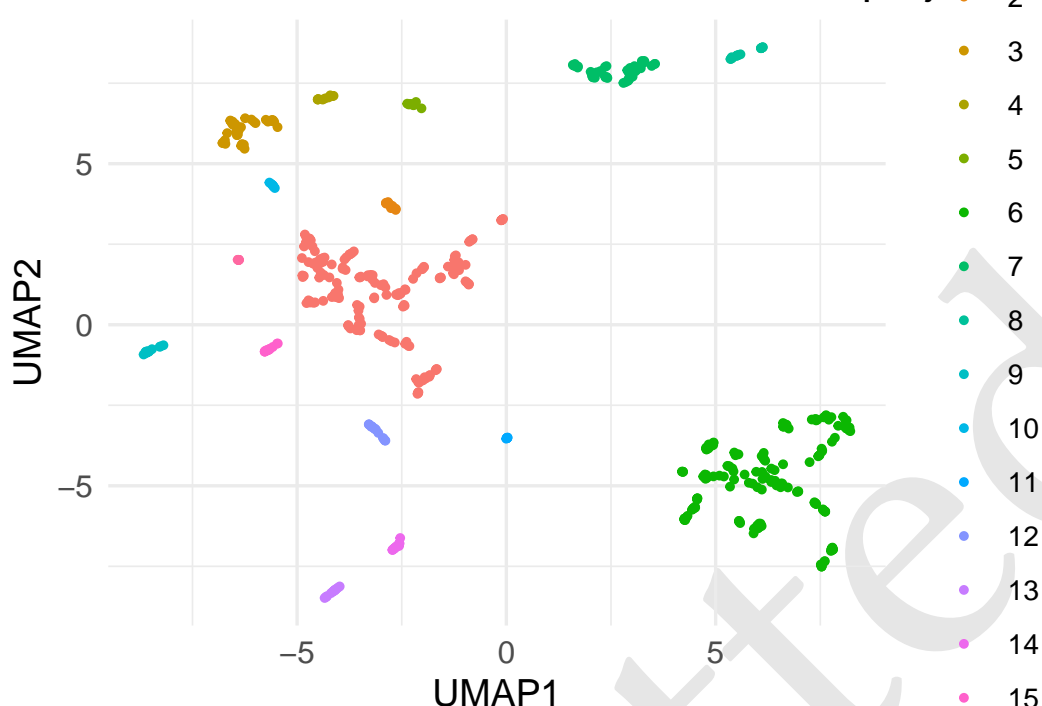


Figure 7: Clustering of High-Risk Drug Cocktails Identified by the Genetic Algorithm on the FAERS dataset. This Figure allows to see proximity between multiple clusters and better understand why some cluster exhibits similarities.

- R (Drugs per Report): The number of medications listed in a single patient report. On our data the mean size of drug cocktails per patient is approximately 2.2. Because K and R are bounded, the complexity simplifies to $O(N)$ per candidate evaluation.

6 Code and Results

See the complete results of application of methodology on the FAERS dataset [on this link](#).

Code to reproduce the experiments conducted in this article can be found here :

- GitHub link of the data refinement code : [JulesBa-Git/FAERS-xml-parser](#).
- GitHub link to the latest release of the R package of the complete methodology : [JulesBa-Git/emcAdr](#).
- The code of the methodology is also available on the [CRAN](#).
- The code to obtain figures is available on the `figures/scripts` folder of this repository.

References

- Ahmed, Ismail, Cyril Dalmaso, Françoise Haramburu, Frantz Thiessard, Philippe Broët, and Pascale Tubert-Bitter. 2010. "False Discovery Rate Estimation for Frequentist Pharmacovigilance Signal Detection Methods." *Biometrics* 66 (1): 301–9.
- Almenoff, June, Joseph M Tonning, A Lawrence Gould, Ana Szarfman, Manfred Hauben, Rita Ouellet-Hellstrom, Robert Ball, et al. 2005. "Perspectives on the Use of Data Mining in Pharmacovigilance." *Drug Safety* 28 (11): 981–1007.

- 577 Au, Siu-Kui, and James L Beck. 2001. "Estimation of Small Failure Probabilities in High Dimensions
578 by Subset Simulation." *Probabilistic Engineering Mechanics* 16 (4): 263–77.
- 579 Bangard, Jules. 2025. *The emcAdr Package*. <https://cran.r-project.org/web/packages/emcAdr/>.
- 580 Bate, Andrew, and Stephen JW Evans. 2009. "Quantitative Signal Detection Using Spontaneous ADR
581 Reporting." *Pharmacoepidemiology and Drug Safety* 18 (6): 427–36.
- 582 Bate, Andrew, Marie Lindquist, I Ralph Edwards, Sten Olsson, Roland Orre, Anders Lansner, and
583 R Melhado De Freitas. 1998. "A Bayesian Neural Network Method for Adverse Drug Reaction
584 Signal Generation." *European Journal of Clinical Pharmacology* 54: 315–21.
- 585 Candore, Gianmario, Kristina Juhlin, Katrin Manlik, Bharat Thakrar, Naashika Quarcoo, Suzie
586 Seabroke, Antoni Wisniewski, and Jim Slattery. 2015. "Comparison of Statistical Signal Detection
587 Methods Within and Across Spontaneous Reporting Databases." *Drug Safety* 38 (6): 577–87.
- 588 Dechanont, Supinya, Sirada Maphanta, Bodin Butthum, and Chuenjid Kongkaew. 2014. "Hospital
589 Admissions/Visits Associated with Drug–Drug Interactions: A Systematic Review and Meta-
590 Analysis." *Pharmacoepidemiology and Drug Safety* 23 (5): 489–97.
- 591 Ducloux, D, V Schuller, C Bresson-Vautrin, and JM Chalopin. 1997. "Colchicine Myopathy in Renal
592 Transplant Recipients on Cyclosporin." *Nephrology, Dialysis, Transplantation: Official Publication
593 of the European Dialysis and Transplant Association-European Renal Association* 12 (11): 2389–92.
- 594 DuMouchel, William. 1999. "Bayesian Data Mining in Large Frequency Tables, with an Application
595 to the FDA Spontaneous Reporting System." *The American Statistician* 53 (3): 177–90.
- 596 Ester, Martin, Hans-Peter Kriegel, Jörg Sander, Xiaowei Xu, et al. 1996. "A Density-Based Algorithm
597 for Discovering Clusters in Large Spatial Databases with Noise." In *Kdd*, 96:226–31. 34.
- 598 Evans, Stephen JW, Patrick C Waller, and S Davis. 2001. "Use of Proportional Reporting Ratios (PRRs)
599 for Signal Generation from Spontaneous Adverse Drug Reaction Reports." *Pharmacoepidemiology
600 and Drug Safety* 10 (6): 483–86.
- 601 Firth, David. 1993. "Bias Reduction of Maximum Likelihood Estimates." *Biometrika* 80 (1): 27–38.
- 602 Fusaroli, Michele, Valentina Giunchi, Vera Battini, Stefano Puligheddu, Charles Khouri, Carla
603 Carnovale, Emanuel Raschi, and Elisabetta Poluzzi. 2024. "Enhancing Transparency in Defining
604 Studied Drugs: The Open-Source Living DiAna Dictionary for Standardizing Drug Names in the
605 FAERS." *Drug Safety*, 1–14.
- 606 Gosho, Masahiko, Kazushi Maruo, Keisuke Tada, and Akihiro Hirakawa. 2017. "Utilization of
607 Chi-Square Statistics for Screening Adverse Drug-Drug Interactions in Spontaneous Reporting
608 Systems." *European Journal of Clinical Pharmacology* 73: 779–86.
- 609 Grossmann, Steffen, Sebastian Bauer, Peter N Robinson, and Martin Vingron. 2007. "Improved
610 Detection of Overrepresentation of Gene-Ontology Annotations with Parent–Child Analysis."
611 *Bioinformatics* 23 (22): 3024–31.
- 612 Hall, Mederic M, Jonathan T Finnoff, and Jay Smith. 2011. "Musculoskeletal Complications of
613 Fluoroquinolones: Guidelines and Precautions for Usage in the Athletic Population." *PM&R* 3 (2):
614 132–42.
- 615 Hauben, Manfred. 2023. "Artificial Intelligence and Data Mining for the Pharmacovigilance of
616 Drug–Drug Interactions." *Clinical Therapeutics* 45 (2): 117–33.
- 617 Heijden, Peter GM van der, Eugène P van Puijenbroek, Stef van Buuren, and Jacques W Van der
618 Hofstede. 2002. "On the Assessment of Adverse Drug Reactions from Spontaneous Reporting
619 Systems: The Influence of Under-Reporting on Odds Ratios." *Statistics in Medicine* 21 (14):
620 2027–44.
- 621 Heinze, Georg, Meinhard Ploner, and Meinhard Dunkler. 2023. *Logistf: Firth's Penalized Likelihood
622 Logistic Regression*. <https://CRAN.R-project.org/package=logistf>.
- 623 Heo, Seok-Jae, Sohee Jeong, Dageom Jung, and Inkyung Jung. 2024. "Signal Detection Statistics of
624 Adverse Drug Events in Hierarchical Structure for Matched Case–Control Data." *Biostatistics* 25
625 (4): 1112–21.
- 626 Ibrahim, Heba, A Abdo, Ahmed M El Kerdawy, and A Sharaf Eldin. 2021. "Signal Detection in

627 Pharmacovigilance: A Review of Informatics-Driven Approaches for the Discovery of Drug-Drug
628 Interaction Signals in Different Data Sources.” *Artificial Intelligence in the Life Sciences* 1: 100005.

629 Ibrahim, Heba, Amr Saad, Amany Abdo, and A Sharaf Eldin. 2016. “Mining Association Patterns
630 of Drug-Interactions Using Post Marketing FDA’s Spontaneous Reporting Data.” *Journal of*
631 *Biomedical Informatics* 60: 294–308.

632 Kulldorff, Martin, Zixing Fang, and Stephen J Walsh. 2003. “A Tree-Based Scan Statistic for Database
633 Disease Surveillance.” *Biometrics* 59 (2): 323–31.

634 Levenshtein, Vladimir I et al. 1966. “Binary Codes Capable of Correcting Deletions, Insertions, and
635 Reversals.” In *Soviet Physics Doklady*, 10:707–10. 8. Soviet Union.

636 McInnes, Leland, John Healy, and James Melville. 2018. “Umap: Uniform Manifold Approximation
637 and Projection for Dimension Reduction.” *arXiv Preprint arXiv:1802.03426*.

638 Medicines and Healthcare products Regulatory Agency. 2014. “Domperidone: Risks of Cardiac Side
639 Effects.” *Drug Safety Update* 7 (10): A1. [https://www.gov.uk/drug-safety-update/domperidone-
640 risks-of-cardiac-side-effects](https://www.gov.uk/drug-safety-update/domperidone-risks-of-cardiac-side-effects).

641 Miernik, Sebastian, Agata Matusiewicz, and Marzena Olesińska. 2024. “Drug-Induced Myopathies: A
642 Comprehensive Review and Update.” *Biomedicines* 12 (5): 987.

643 Noguchi, Yoshihiro, Keisuke Aoyama, Satoaki Kubo, Tomoya Tachi, and Hitomi Teramachi. 2020.
644 “Improved Detection Criteria for Detecting Drug-Drug Interaction Signals Using the Proportional
645 Reporting Ratio.” *Pharmaceuticals* 14 (1): 4.

646 Noguchi, Yoshihiro, Anri Ueno, Manami Otsubo, Hayato Katsuno, Ikuto Sugita, Yuta Kanematsu,
647 Aki Yoshida, Hiroki Esaki, Tomoya Tachi, and Hitomi Teramachi. 2018. “A New Search Method
648 Using Association Rule Mining for Drug-Drug Interaction Based on Spontaneous Report System.”
649 *Frontiers in Pharmacology* 9: 197.

650 Norén, G Niklas, Rolf Sundberg, Andrew Bate, and I Ralph Edwards. 2008. “A Statistical Methodology
651 for Drug–Drug Interaction Surveillance.” *Statistics in Medicine* 27 (16): 3057–70.

652 Pariente, Antoine, Fleur Gregoire, Annie Fourrier-Reglat, Françoise Haramburu, and Nicholas Moore.
653 2007. “Impact of Safety Alerts on Measures of Disproportionality in Spontaneous Reporting
654 Databases the Notoriety Bias.” *Drug Safety* 30 (10): 891–98.

655 Pétrowski, Alain, and Sana Ben-Hamida. 2017. *Evolutionary Algorithms*. John Wiley & Sons.

656 Puijtenbroek, Eugene P. van, Andrew Bate, Hubert G. M. Leufkens, Marie Lindquist, Roland Orre,
657 and Antoine C. G. Egberts. 2002. “A Comparison of Measures of Disproportionality for Signal
658 Detection in Spontaneous Reporting Systems for Adverse Drug Reactions.” *Pharmacoepidemiology*
659 *and Drug Safety* 11. <https://api.semanticscholar.org/CorpusID:21212215>.

660 Puijtenbroek, Eugène P van, Antoine CG Egberts, Eibert R Heerdink, and Hubert GM Leufkens. 2000.
661 “Detecting Drug–Drug Interactions Using a Database for Spontaneous Adverse Drug Reactions:
662 An Example with Diuretics and Non-Steroidal Anti-Inflammatory Drugs.” *European Journal of*
663 *Clinical Pharmacology* 56: 733–38.

664 Robert, Christian P., and George Casella. 2004. “The Metropolis–Hastings Algorithm.” In *Monte*
665 *Carlo Statistical Methods*, 267–320. New York, NY: Springer New York. [https://doi.org/10.1007/978-
666 1-4757-4145-2_7](https://doi.org/10.1007/978-1-4757-4145-2_7).

667 Sanson-Fisher, Robert William, Billie Bonevski, Lawrence W Green, and Cate D’Este. 2007. “Limita-
668 tions of the Randomized Controlled Trial in Evaluating Population-Based Health Interventions.”
669 *American Journal of Preventive Medicine* 33 (2): 155–61.

670 Schuler, Jochen, Christina Dückelmann, Wolfgang Beindl, Erika Prinz, Thomas Michalski, and Max
671 Pichler. 2008. “Polypharmacy and Inappropriate Prescribing in Elderly Internal-Medicine Patients
672 in Austria.” *Wiener Klinische Wochenschrift* 120.

673 Tekin, Elif, Cynthia White, Tina Manzhong Kang, Nina Singh, Mauricio Cruz-Loya, Robert Damoiseaux,
674 Van M. Savage, and Pamela J. Yeh. 2018. “Prevalence and Patterns of Higher-Order Drug
675 Interactions in Escherichia Coli.” *Npj Systems Biology and Applications* 4 (1): 31. [https://doi.org/
676 10.1038/s41540-018-0069-9](https://doi.org/10.1038/s41540-018-0069-9).

677 Valiyil, Ritu, and Lisa Christopher-Stine. 2010. "Drug-Related Myopathies of Which the Clinician
678 Should Be Aware." *Current Rheumatology Reports* 12: 213–20.

679 Van Puijenbroek, Eugène P, Antoine CG Egberts, Ronald HB Meyboom, and Hubert GM Leufkens.
680 1999. "Signalling Possible Drug–Drug Interactions in a Spontaneous Reporting System: Delay of
681 Withdrawal Bleeding During Concomitant Use of Oral Contraceptives and Itraconazole." *British
682 Journal of Clinical Pharmacology* 47 (6): 689–93.

683 Wang, Xueying, Lang Li, Lei Wang, Weixing Feng, and Pengyue Zhang. 2020. "Propensity Score-
684 Adjusted Three-Component Mixture Model for Drug-Drug Interaction Data Mining in FDA
685 Adverse Event Reporting System." *Statistics in Medicine* 39 (7): 996–1010.

686 Session information

687 R version 4.5.1 (2025-06-13)
688 Platform: aarch64-apple-darwin20
689 Running under: macOS Tahoe 26.1
690
691 Matrix products: default
692 BLAS: /Library/Frameworks/R.framework/Versions/4.5-arm64/Resources/lib/libRblas.0.dylib
693 LAPACK: /Library/Frameworks/R.framework/Versions/4.5-arm64/Resources/lib/libRlapack.dylib; LAPACK
694
695 locale:
696 [1] fr_FR/UTF-8/fr_FR/C/fr_FR/fr_FR
697
698 time zone: Europe/Oslo
699 tzcode source: internal
700
701 attached base packages:
702 [1] stats graphics grDevices datasets utils methods base
703
704 other attached packages:
705 [1] stringr_1.6.0 umap_0.2.10.0 ggplot2_3.5.2 dbscan_1.2.2 dplyr_1.1.4
706 [6] emcAdr_1.2
707
708 loaded via a namespace (and not attached):
709 [1] Matrix_1.7-3 gtable_0.3.6 jsonlite_2.0.0 compiler_4.5.1
710 [5] renv_1.1.5 tinytex_0.57 tidyselect_1.2.1 Rcpp_1.1.0
711 [9] png_0.1-8 scales_1.4.0 yaml_2.3.10 fastmap_1.2.0
712 [13] reticulate_1.43.0 lattice_0.22-7 R6_2.6.1 labeling_0.4.3
713 [17] generics_0.1.4 knitr_1.50 tibble_3.3.0 openssl_2.3.3
714 [21] pillar_1.11.0 RColorBrewer_1.1-3 rlang_1.1.6 stringi_1.8.7
715 [25] xfun_0.52 cli_3.6.5 withr_3.0.2 magrittr_2.0.3
716 [29] digest_0.6.37 grid_4.5.1 askpass_1.2.1 lifecycle_1.0.4
717 [33] vctr_0.6.5 RSpecra_0.16-2 evaluate_1.0.4 glue_1.8.0
718 [37] farver_2.1.2 rmarkdown_2.29 tools_4.5.1 pkgconfig_2.0.3
719 [41] htmltools_0.5.8.1